Atmospheric
Chemistry
and Physics

# Estimating regional greenhouse gas fluxes: an uncertainty analysis of planetary boundary layer techniques and bottom-up inventories

**X. Zhang[1,*], X. Lee[1,2], T. J. Griffis[3], J. M. Baker[4], and W. Xiao[2]**

[1]School of Forestry and Environmental Studies, Yale University, New Haven, CT, USA
[2]Yale-NUIST Center on Atmospheric Environment, Nanjing University of Information Science and Technology, Nanjing, Jiangsu, China
[3]Department of Soil, Water, and Climate, University of Minnesota, Saint Paul, MN, USA
[4]Agricultural Research Service, USDA, Saint Paul, MN, USA
[*]now at: Woodrow Wilson School of Public and International Affairs, Princeton University, Princeton, NJ, USA

*Correspondence to:* X. Zhang (zhangxin.yale@gmail.com)

**Abstract.** Quantification of regional greenhouse gas (GHG) fluxes is essential for establishing mitigation strategies and evaluating their effectiveness. Here, we used multiple top-down approaches and multiple trace gas observations at a tall tower to estimate regional-scale GHG fluxes and evaluate the GHG fluxes derived from bottom-up approaches. We first applied the eddy covariance, equilibrium, inverse modeling (CarbonTracker), and flux aggregation methods using 3 years of carbon dioxide ($CO_2$) measurements on a 244 m tall tower in the upper Midwest, USA. We then applied the equilibrium method for estimating $CH_4$ and $N_2O$ fluxes with 1-month high-frequency $CH_4$ and $N_2O$ gradient measurements on the tall tower and 1-year concentration measurements on a nearby tall tower, and evaluated the uncertainties of this application. The results indicate that (1) the flux aggregation, eddy covariance, the equilibrium method, and the CarbonTracker product all gave similar seasonal patterns of the regional $CO_2$ flux ($10^5$–$10^6$ km$^2$), but that the equilibrium method underestimated the July $CO_2$ flux by 52–69 %. (2) The annual budget varied among these methods from $-54$ to $-131$ g C–$CO_2$ m$^{-2}$ yr$^{-1}$, indicating a large uncertainty in the annual $CO_2$ flux estimation. (3) The regional $CH_4$ and $N_2O$ emissions according to a top-down method were at least 6 and 2 times higher than the emissions from a bottom-up inventory (Emission Database for Global Atmospheric Research), respectively. (4) The global warming potentials of the $CH_4$ and $N_2O$ emissions were equal in magnitude to the cooling benefit of the regional $CO_2$ uptake. The regional GHG budget, including both biological and anthropogenic origins, is estimated at $7 \pm 160$ g $CO_2$ equivalent m$^{-2}$ yr$^{-1}$.

## 1 Introduction

Although quantifying greenhouse gas (GHG) fluxes at the regional scale ($10^2$–$10^6$ km$^2$) is essential for coordinating GHG mitigation strategies, observations and flux information at these relevant scales are still extremely limited (e.g., Chen et al., 2008; Nisbet and Weiss, 2010). To fill this scale gap, some researchers build ecosystem models and aggregate the modeled flux according to land information (e.g., Desai et al., 2008; Tang et al., 2012; Xiao et al., 2008), while others use GHG concentration observations in combination with atmospheric transport models to derive the land surface flux (Lauvaux et al., 2012; Peters et al., 2007). The aggregation method is a bottom-up approach. Another bottom-up method is the IPCC national GHG inventory system (IPCC, 2006) based on emission factors and data concerning anthropogenic activities. The bottom-up applications are relatively easy to implement; however, they require independent verification because uncertainties in land cover, anthropogenic activity, vegetation flux, and emission factors can lead to large biases (Chen et al., 2008; Levy et al., 1999). Hence, there is a strong motivation for using top-down methods to provide an independent constraint on the regional fluxes.

There are several top-down methods for estimating regional GHG fluxes, including tall-tower eddy covariance (Davis et al., 2003), the equilibrium boundary layer approach (Bakwin et al., 2004; Betts et al., 2004; Desai et al., 2010; Helliker et al., 2004), and inverse modeling (Peters et al., 2007). Each method uses different assumptions, has inherent advantages and disadvantages, and is sensitive to different parameters. Eddy covariance (EC) provides a direct measurement of the flux, using measurement of the wind fluctuations and the scalar of interest. Eddy covariance has been used for $CO_2$ flux measurement on tall towers (Davis et al., 2003; Haszpra et al., 2005), while few tall-tower flux observations of $CH_4$ and $N_2O$ have been carried out due to instrument limitations (Desai et al., 2012) and the relatively large uncertainty for these measurements (20–300 % for $CH_4$, 30–1800 % for $N_2O$) (Kroon et al., 2010). Based on the mass balance in the atmospheric boundary layer, the equilibrium method assumes that the exchange at the top of the boundary layer and the exchange at the land surface are in equilibrium over periods longer than about 1 month (Betts, 2000). The largest source of uncertainty of this method lies in determining the background concentration above the boundary layer and the entrainment rate at the top of the boundary layer. Inverse modeling determines the land surface flux by using atmospheric transport models that are constrained by observed trace gas concentrations. The prior land surface flux, land surface observations, the meteorological inputs, and atmospheric transportation schemes are all important for determining the accuracy of the modeled flux (Peters et al., 2007). As a result, the deficiency in any of these four factors can limit the accuracy of the model.

In this study, we used several top-down approaches to evaluate the bottom-up fluxes of $CO_2$, $CH_4$, and $N_2O$ for a region dominated by agriculture. The intercomparison of multiple techniques was used to identify systematic biases of each method and constrain the overall uncertainties. We first used $CO_2$ to evaluate the equilibrium boundary layer method against tall-tower eddy covariance, flux aggregation, and the flux produced by an inverse model. We then applied the equilibrium method to estimate the $CH_4$ and $N_2O$ fluxes. The final task was to compare the $CH_4$ and $N_2O$ fluxes with two bottom-up emission inventories: (1) EDGAR42 (European Commission, Joint Research Centre (JRC) and the Netherlands Environmental Assessment Agency (PBL), Emission Database for Global Atmospheric Research (EDGAR), release version 4.2, http://edgar.jrc.ec.europa.eu, 2011), an inventory data set used widely in atmospheric models (Jeong et al., 2012); and (2) a national GHG inventory developed by the US Environmental Protection Agency (US EPA, 2014).

## 2 Data and methods

### 2.1 Research site

The boundary layer observations were made on a 244 m communication tower (KCMP tower) located at the Rosemount Research and Outreach Center, University of Minnesota, about 25 km south of Minneapolis/Saint Paul (44°41′19″ N, 93°4′22″ W). According to the US Department of Agriculture Cropland Data Layer data in 2009, the landscape around the tall tower was dominated by cropland, which accounted for 41 % of the land cover within a 10 km radius of the tower and 37 % within a 600 km radius. Corn and soybean were the dominant crop species, accounting for 55 and 38 % of the cropland, respectively. About 40 % of the land within the 600 km radius was covered by forest, grassland and pasture. The other land use was comprised of developed land, wetland, and open water. The land cover pattern described here for 2009 had a smaller corn-to-soybean ratio than that reported by Griffis et al. (2010) for 2007. This difference was mainly attributed to more corn plantation in 2007 stimulated by increased ethanol biofuel demand.

### 2.2 Mixing ratio data

$CO_2$ mixing ratios at the 32, 56, 100, and 200 m heights above the ground were measured by a tunable diode laser analyzer (TDL) (model TGA 100A, Campbell Scientific Inc., Logan, UT, USA) (Griffis et al., 2010). Air at these levels was drawn down by a pump (model DOA-V502A-FB, Gast Group Inc., Benton Harbor, MI, USA) through four Synflex tubes (6.25 mm ID) at a line pressure of 60 kPa and at a flow rate of 16 L min$^{-1}$. The air was sampled sequentially, each for 30 s. The sampled air was dried prior to analysis using a Nafion drier and brought to a common temperature. The $CO_2$ measurement was calibrated for every measurement cycle against the National Oceanic and Atmospheric Administration, Earth System Research Laboratory (NOAA-ESRL) standards. The hourly precision of the $CO_2$ measurement was approximately 0.03 ppm.

In addition, an intensive campaign was carried out from 30 August to 25 September (DOY 243–269), 2009. During this campaign, we measured $CO_2$, $H_2O$, $CH_4$, and $N_2O$ mixing ratios at the 200 and 3 m heights on the tower. Air was drawn from these heights at a flow rate of 1.3 L min$^{-1}$ and 0.9 L min$^{-1}$, respectively, through two Synflex tubes (6.25 mm ID). A portion (0.6 L min$^{-1}$) of this flow was delivered to an infrared gas analyzer (IRGA model LI-6262, LI-COR, Lincoln, NE, USA) for $CO_2$ and $H_2O$ mixing ratio measurements, and a small amount (180 mL min$^{-1}$) was delivered to another TDL for $CH_4$ and $N_2O$ measurements. Measurement precisions for $CO_2$, $CH_4$, and $N_2O$ were 0.2 ppm, 1.2 ppb, and 0.5 ppb, respectively. The IRGA was manually calibrated with a standard $CO_2$ gas (391.03 ± 0.03 ppm) and a dew point generator

(LI-610, LI-COR) at the beginning of the experiment. The accuracy of its measurement was improved in post-field-analysis by adding offsets so that its 200 m reading matched that registered by the TDL $CO_2$ analyzer for the same height. The TDL for $N_2O$ and $CH_4$ measurement was plumbed to a four-port manifold that used a switching sequence on the order of 200 m, 3 m, calibration zero, and calibration span, with 30 s spent on each port and the first 15 s after each switching omitted from the analysis. The $N_2O$ concentration of the calibration span was traceable to a NOAA-ESRL gold standard. The $CH_4$ concentration of the calibration span was calibrated against a known standard provided by a local supplier and was also traceable to the NOAA-ESRL standard scale.

## 2.3 Eddy covariance data

A closed-path EC system installed at the height of 100 m on the tower was used to measure the $CO_2$ flux from 2007 to 2009 (Griffis et al., 2010). This system consisted of a 3-D sonic anemometer/thermometer (model CSAT3, Campbell Scientific Inc.) and the TDL analyzer (model TGA 100A, Campbell Scientific) for $CO_2$ concentration. The sample tubing was 125 m long (6.25 mm ID, Synflex), which resulted in a typical lag time of 11 s, with Reynolds numbers exceeding 3500. Fluctuations in the velocities and concentrations were recorded at 10 Hz, and a block averaging time of 60 min was used to capture the dominant flux-containing frequencies.

Further, in 2009 two closed-path eddy covariance systems were used at two 10 m towers in the middle of corn (G21) and soybean fields (G19) (Baker and Griffis, 2005) about 3 km away from the tall tower. They recorded half-hourly fluxes of $CO_2$ and $H_2O$.

## 2.4 Top-down flux estimation methods

### 2.4.1 Tall-tower eddy covariance

Briefly, the tall-tower $CO_2$ flux was determined as the sum of the eddy covariance term measured at the 100 m height ($\overline{w'c'}$) and the storage term between the land surface and this height ($F_S$).

$$F_{EC} = \overline{w'c'} + F_S \qquad (1)$$

Here, we assume that horizontal and vertical advection were negligible (Davis et al., 2003; Griffis et al., 2010). Wind statistics and fluxes were transformed into the planar fit coordinate system (Lee et al., 2004). Eddy fluxes were computed using the maximum covariance method with strict limits on window size based on manifold pressure and flow rates. Flux losses attributed to a combination of sensor separation, sonic path averaging, tube attenuation, and block averaging were estimated using the analytical model of Massman (2000). These losses typically ranged between 5 and 20 %. A detailed description of the eddy covariance system and flux calculation can be found in Griffis et al. (2010).

The eddy covariance method does not perform well in stable atmospheric conditions, and friction velocity ($u_*$) is commonly used as a quality control for such conditions (Davis et al., 2003; Goulden et al., 1996). In this study, we discarded the nighttime flux data when $u_*$ was less than $0.10\,\mathrm{m\,s^{-1}}$, which is a threshold often used for agricultural environments (Baker and Griffis, 2005; Griffis et al., 2005).

Large negative fluxes in the early morning have been observed at many eddy covariance tower sites, and it may lead to an overestimation of $CO_2$ uptake during the growing season by as much as 20 % (Anthoni et al., 1999; Davis et al., 2003; Yi et al., 2000). Davis et al. (2003) suggested that this bias is caused by horizontal and vertical advection, and it can be corrected by excluding the negative $CO_2$ flux that exceeds a pre-defined level. In this study, we excluded the morning (06:00 and 10:00 LST) data when the storage term was large (i.e., $F_S < -4\,\mu\mathrm{mol\,m^{-2}\,s^{-1}}$). This storage term screening reduced the estimated $CO_2$ uptake during the growing season (May to September) by 18 % and is consistent with that reported in the literature (Davis et al., 2003; Yi et al., 2000). Details about the calculation of the storage term and a discussion about the data-screening standard for the negative storage term in early morning is reported in the Supplement (Sect. S1).

The monthly $CO_2$ flux was determined by the mean of the composite diurnal variation of the $CO_2$ flux. In 2009, excluding the malfunctioning of the instrumentation, the available data was 78 %. The $u_*$ and storage term screening eliminated an additional 12 and 2 % of the data, respectively. We estimated the monthly mean from the diurnal composite of the $CO_2$ flux based on valid observations (Sect. S2 in Supplement).

### 2.4.2 Equilibrium method

The equilibrium method (EQ) provides a way to quantify regional trace gas fluxes from mixing ratio measurements in the boundary layer (Bakwin et al., 2004; Betts, 2000; Betts et al., 2004; Denmead et al., 1996; Desai, 2010; Helliker et al., 2004; Williams et al., 2011). So far, this method has been applied to $CO_2$ and $N_2O$ (Griffis et al., 2013) but not to $CH_4$. The EQ method assumes that, over relatively long timescales (weeks), the diurnal dynamics of boundary layer processes can be ignored and the boundary layer reaches statistical equilibrium (Griffis et al., 2013; Helliker et al., 2004). Therefore, the averaged horizontal advection and storage are negligible in the boundary layer budget (Williams et al., 2011) and the land surface flux ($F_{Eq}$) is in balance with the exchange at the top of the boundary layer as

$$F_{Eq} = \rho W (c_+ - c_m), \qquad (2)$$

where $c_+$ and $c_m$ are the mixing ratio of $CO_2$, $CH_4$, or $N_2O$ above and within the boundary layer, respectively, and $\rho$ and $W$ are air density and the vertical velocity, respectively, at the top of boundary layer. Here, $c_+$ was assumed as the

concentration measured at Niwot Ridge (NWR, $40°3'11''$ N, $105°35'10''$ W) CO, USA, which is the closest background site operated by NOAA (Conway et al., 1994) and is upwind of KCMP tower in the Ferrel cell. $c_m$ was the concentration at 200 m measured by TDL analyzers and calibrated to the NOAA-ESRL standards. The concentrations used in the calculation were the composite diurnal variations for each month in the case of $CO_2$ and the diurnal composites for the intensive campaign in the case of $CH_4$ and $N_2O$. The equilibrium method was used for calculating the $CO_2$ flux from 2007 to 2009. However, due to availability of data, the comparison among methods is limited to the 2009 $CO_2$ fluxes.

We used the following two methods to determine $\rho W$ (Helliker et al., 2004) for the three GHGs:

$$\rho W = \frac{F_w}{c_{w,+} - c_{w,m}}, \qquad (3)$$

$$\rho W = -\frac{\Omega}{g \cdot M_{air}}, \qquad (4)$$

where $F_w$ and $c_{w,m}$ are the water vapor flux and mixing ratio measured at 100 m and 200 m on the tall tower, respectively, $c_{w,+}$ and $\Omega$ are the water vapor mixing ratio and the pressure vertical velocity (in units of $Pa\,s^{-1}$) at the 700 hPa level in the National Centers for Environmental Prediction and the National Center for Atmospheric Research (NCEP/NCAR) Reanalysis-2 data, $g$ is gravitational acceleration, and $M_{air}$ is molecular mass of dry air ($g\,mol^{-1}$). $\rho W$ calculated from Eq. (3) is essentially the same as for Eq. (4) under the EQ assumptions because large-scale synoptic subsidence dominates the exchange at the top of the boundary layer (Helliker et al., 2004). In addition, for $CH_4$ and $N_2O$, we also used $CO_2$ as a tracer to determine $\rho W$:

$$\rho W = \frac{F_C}{c_{C,+} - c_{C,m}}, \qquad (5)$$

where $F_C$ is the $CO_2$ flux measured by the EC system on the tall tower, $c_{C,+}$ and $c_{C,m}$ are the $CO_2$ mixing ratio measured at the NWR background site and at the 200 m level on the tall tower, respectively.

### 2.4.3   Inverse modeling

We used the $CO_2$ flux product from the global inversion model CarbonTracker 2011_oi (CT) (Peters et al., 2007 with updates documented at http://carbontracker.noaa.gov) as a reference to compare with the flux determined with the methods described above. This product provides 3-hourly $CO_2$ fluxes from 2000–2010 at a spatial resolution of 1° by 1°, so the number of grid points within the 100, 200, 300, and 600 km radii of the tall tower is 2, 10, 25, and 90, respectively.

The inversion $CO_2$ flux consists of fossil fuel burning, fire, land, and ocean flux. The $CO_2$ flux from fossil fuel was the average of two fossil fuel $CO_2$ emission data sets: one is the legacy CarbonTracker fossil fuel product using the global total from the Carbon Dioxide Information and Analysis Center (CDIAC, Boden et al. 2011) and the spatial distribution from EDGAR; and the other is the Odiac (Open-source Data Inventory for Anthropogenic $CO_2$) emission product reported by Oda and Maksyutov (2011).

### 2.5   Flux aggregation (FA)

The regional trace gas flux ($F_{FA}$) can be estimated by aggregating sectorial and spatial fluxes using sectorial statistics and land cover information (Chen et al., 2008; Desai et al., 2008; Nisbet and Weiss, 2010; Tang et al., 2012). The total $CO_2$ flux from the landscape is the sum of the anthropogenic flux and biological flux. In this study, the anthropogenic flux ($F_{ant}$) was the prescribed fossil fuel flux in the CarbonTracker product for a target region. The biological flux was calculated by aggregating the $CO_2$ flux from six major land cover types.

$$F_{FA} = F_{ant} + \sum_{i=1}^{6} frac_i \cdot F_{bio,i} \qquad (6)$$

In this equation, $frac_i$ is the fraction of land cover type $i$ for a target region, and $F_{bio,i}$ is the $CO_2$ flux from land cover type $i$. The six land cover types are cropland (corn and soybean), forest, grassland/pasture, wetland, open water, and developed land.

In order to compare with the fluxes from top-down methods, we estimated the bottom-up flux using the flux aggregation (FA) method within the tall tower footprint. Various methods have been developed for determining the footprint of the concentration or eddy flux measurement (Chen et al., 2009; Kljun et al., 2004; Lin et al., 2003; Vesala et al., 2008). We used two footprint methods. The first method is based on determining an equally weighted circular footprint centered at the tall tower. This method assumes that the area within each circular footprint has the same influence on the flux measured at the tall tower despite its distance from the tower, and therefore, $frac_i$ is the fraction of land cover type $i$ within a certain radius around the tall tower. We tested the radii from 5 to 600 km because the fetch of the EC flux footprint is thought to be 10 (during strong convection) to 100 (during neutral or stable conditions) times the measurement height (Horst and Weil, 1992; Davis et al., 2003); however, some studies also suggest that the fetch-to-measurement-height ratio is much higher than 100 when the flux is measured at a high level (e.g., higher than 20 m) (Gash, 1986; Leclerc and Thurtell, 1990). The second footprint method we applied derives the footprint from the Stochastic Time-Inverted Lagrangian Transport model (STILT, Lin et al., 2003). During September, when the intensive campaign was carried out, we released 100 air parcels hourly at the tower and transported these parcels backward for 2 days. The distribution of the air parcels determined the tall tower footprint. (This footprint
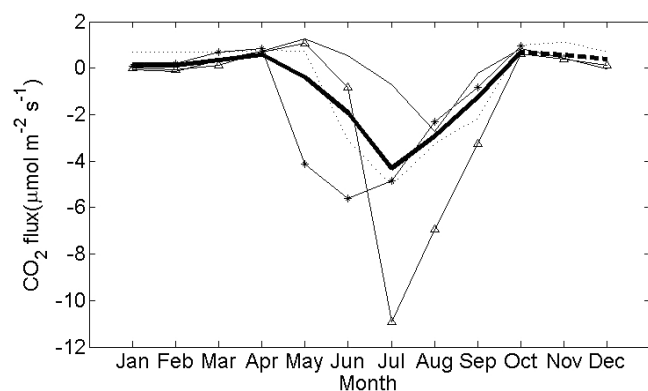
**Figure 1.** The biogenic $CO_2$ flux (thick solid line) from the landscape around the tall tower, calculated from monthly averages of $CO_2$ flux from major land cover types. The fluxes for corn (solid line with triangles) and soybean (thin solid line) were measured with eddy covariance tower at the G21 and G19 sites near the tall tower in Minnesota. The fluxes for forest (dotted line) and grassland (solid line with stars) were from UMBS and USIB2 AmeriFlux sites in North America.



**Figure 2.** Monthly averages of $CO_2$ flux in 2007 (dotted line), 2008 (dot-dashed line), and 2009 (dashed line) measured with EC on the tall tower. White bars are the mean monthly value from the available data during the 3-year observation period. Error bars on the top of white bars show the lower and upper boundary of the 3-year measurements for each month.

represents the source area of the EQ flux calculated based on the 200 m concentration.) Therefore, $\text{fra}_i$ was determined by overlaying the weighted footprint map with the land cover map. The values of $\text{frac}_i$ from these two different methods are summarized in Table S3 in the Supplement.

The cropland $CO_2$ flux was the weighted average of the flux measured with EC in a soybean field and a cornfield near the tall tower as described above. The forest $CO_2$ flux was obtained from the AmeriFlux data archive (Level 2 data) for the deciduous forest site at the University of Michigan Biological Station (UMBS), 662 km northeast of the tall tower (Curtis et al., 2005; Schmid et al., 2003). The grassland $CO_2$ flux was also from USIB2 AmeriFlux for Fermi Prairie, Illinois, 503 km southeast of the tower (Gomez-Casanovas et al., 2012). Each of the three land cover types was measured by EC flux towers in 2009, and showed different seasonal patterns of $CO_2$ flux (Fig. 1). The biological $CO_2$ flux from wetland, open water, and developed land was considered as negligible in this study because these three land cover types only accounted for about 20 % of the tall tower footprint, and the reported annual $CO_2$ fluxes from those land cover types were not significantly different from zero or relatively small (Striegl and Michmerhuizen, 1998; Knoll et al., 2013; Olson et al., 2013). For example, Olson et al. (2013) reported that a temperate peatland in northern Minnesota, USA was a small net sink of $CO_2$ in 2009 ($-26.8 \pm 18.7 \, \text{g C–CO}_2 \, \text{m}^{-2} \, \text{yr}^{-1}$), had only about 5 % of the $CO_2$ flux from a cornfield, and about 10 % of the biogenic flux in the tall tower footprint. Considering the land fraction of peatland in the tall tower footprint, the $CO_2$ flux was estimated to be less than 1 % of the biogenic flux.
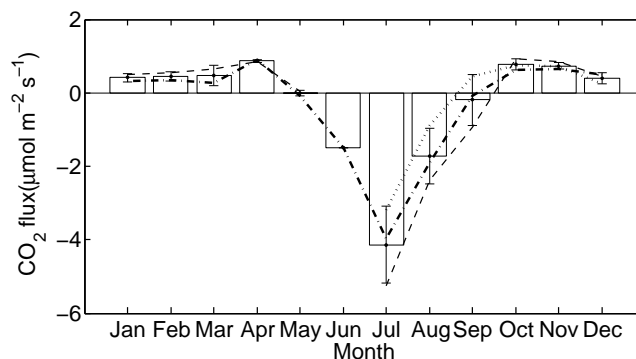
## 3 Results

### 3.1 Constraints on the regional $CO_2$ flux

The tall tower EC $CO_2$ flux exhibits a strong seasonal pattern (Fig. 2). From October to April, the landscape was a net source of $CO_2$, and the averaged efflux was $0.68 \pm 0.10 \, \mu\text{mol m}^{-2} \, \text{s}^{-1}$ (the mean and standard deviation of the three annual values from 2007 to 2009). From May to September, the landscape was a sink of $CO_2$, reaching a peak uptake in July at the rate of $-3.68 \pm 0.99 \, \mu\text{mol m}^{-2} \, \text{s}^{-1}$. There were no monthly mean data for June 2007 and June 2009 due to measurement problems. Since June is the only month that has missing $CO_2$ flux data for 2009, we gap-filled it according to the flux values observed in May to July 2008 and 2009. The annual cumulative flux in 2008 and 2009 was $-24$ and $-131 \, \text{g C–CO}_2 \, \text{m}^{-2} \, \text{yr}^{-1}$, respectively.

In order to test the size of the region that our monthly averaged EC flux represents, we first used CT and FA methods to estimate the $CO_2$ flux with the equally weighted circular footprint for a radius up to 600 km and compared them with the EC flux. The monthly flux values from these methods for the range of radii correlated well with the EC flux ($r > 0.9$, $p < 0.001$) (Table 1), suggesting the land surface flux was relatively homogeneous and was dominated by the seasonal pattern of the biological flux. Further, to test the accuracy of the estimation, the Nash–Sutcliffe efficiency (NSE) was calculated (Nash and Sutcliffe, 1970) as

$$\text{NSE} = 1 - \frac{\sum (o_i - m_i)^2}{\sum (o_i - \overline{o})^2}, \tag{7}$$

where $o_i$ is the EC flux and $m_i$ is the regional mean flux from CT or FA. The summation is performed over all months and the overbar denotes the mean over these months. It is considered a very good fit when $\text{NSE} > 0.75$, and a good fit when
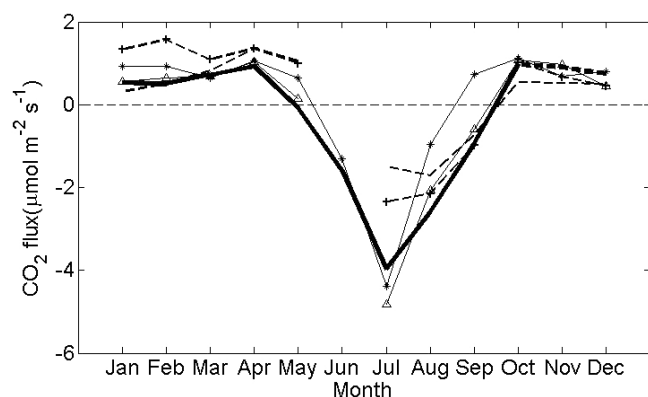
**Figure 3.** Monthly $CO_2$ flux in 2009 estimated with flux aggregation (FA, thick solid line), eddy covariance method ($F_{EC}$, line with triangles), CarbonTracker ($F_{CT}$, line with stars), equilibrium method with $H_2O$ as a tracer ($F_{EH}$, thin dashed line), and equilibrium method using NCEP reanalysis data ($F_{EO}$, thin dashed line with cross). The FA flux ended in October because the grassland data was missing in November and December. The missing FA flux was determined by assuming the missing grassland flux in November and December was the same as October flux (thick dashed line).



**Figure 4.** Hourly averages of $CO_2$ **(a)**, $CH_4$ **(b)**, $N_2O$ **(c)**, and $H_2O$ **(d)** mixing ratios during the observation period from DOY 243 to DOY 269, 2009. Blue solid line – mixing ratio on 200 m. Red dotted line – mixing ratio on 3 m. Black dashed line – mixing ratio at Niwot Ridge site.

$0.65 < \text{NSE} \leq 0.75$ (Moriasi et al., 2007). The results show that the EC flux agrees very well with the regional mean flux from both the CT and FA methods within a 200 km radius or larger (NSE > 0.80). Furthermore, as the radius increased from 200 to 600 km, the CT and FA fluxes did not change significantly. The CT and FA fluxes within a 100 km radius were more positive than the EC flux, mainly due to the strong local anthropogenic emissions from the Minneapolis/Saint Paul urban area. Consequently, for the KCMP tower site, we can consider the EC flux as representing the average flux from a 600 km radius around the tall tower, a typical size of the footprint of tall tower concentration measurement ($10^6$ km²; Gloor et al., 2001).

The aggregated flux based on the STILT footprint was $-1.01 \, \mu\text{mol m}^{-2}\,\text{s}^{-1}$ for the month of September, 2009. In comparison, the EC flux during the same period was $-0.93 \, \mu\text{mol m}^{-2}\,\text{s}^{-1}$, and the FA flux with a 300 and 600 km radius was $-1.04$ and $-0.94 \, \mu\text{mol m}^{-2}\,\text{s}^{-1}$, respectively. The results again confirm that the land cover type around the tower was relatively homogeneous at scales ranging from 200 to 600 km.

Consequently, we consider the tall-tower EC flux as a robust estimate of the regional flux and used it to evaluate the performance of the EQ method. Two $CO_2$ fluxes were determined by the EQ method for each month, one using $H_2O$ as a tracer ($F_{EH}$), calculated with $\rho W$ with Eq. (3), and the other using $\rho W$ in the NCEP reanalysis data ($F_{EO}$, calculated with $\rho W$ with Eq. (4) (Fig. 3). Both $F_{EH}$ and $F_{EO}$ reproduced the seasonal pattern of the EC flux ($r > 0.85$, $p < 0.001$) but significantly underestimated the magnitude of the flux in July.
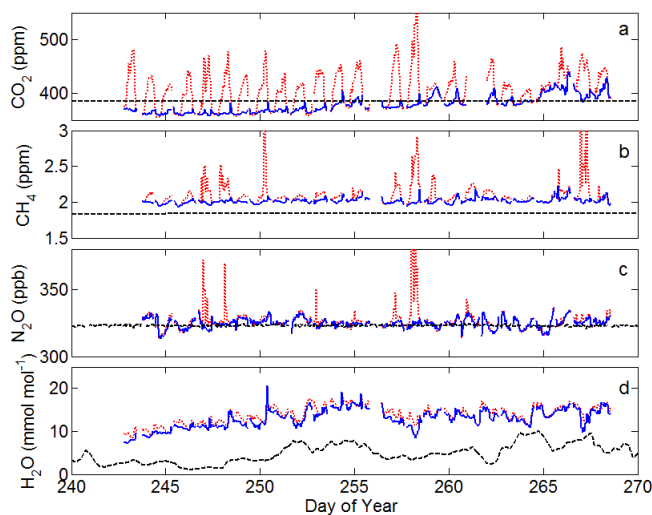
The $F_{EH}$ and $F_{EO}$ fluxes were only 31 and 48 % of the EC flux in July.

### 3.2 GHG concentration patterns

During the intensive campaign, the $CO_2$ mixing ratio at the height of 200 m increased from 365.2 ppm during the first 5 days to 406.2 ppm during the last 5 days (Fig. 4). The mixing ratio changed from below that at the NWR (384.4 ppm) to above that at the NWR site, indicating a transition of the landscape from a $CO_2$ sink to a source. This observation is consistent with the seasonal pattern in the $CO_2$ flux shown in Fig. 3.

The mean $CH_4$ mixing ratio during the observation period was 2.096 and 2.017 ppm at the heights of 3 and 200 m, respectively. The $CH_4$ mixing ratio at both heights was consistently higher than the background mixing ratio at NWR (1.844 ppm), suggesting that the landscape around the tall tower was a $CH_4$ source.

The $N_2O$ mixing ratio during the observation period was also higher than that at NWR. The average $N_2O$ mixing ratios at the heights of 3 and 200 m were 326.7 and 324.8 ppb, which were 4.0 and 2.1 ppb higher than the value at the NWR site (322.7 ppb), respectively, indicating that the landscape was a $N_2O$ source during the observation period.

### 3.3 Regional $CH_4$ and $N_2O$ fluxes

We applied the EQ method in estimating the regional $CH_4$ and $N_2O$ fluxes during the intensive campaign. During this period, $\rho W$ determined with three independent methods (using $CO_2$ and $H_2O$ tracers and the NCEP reanalysis data) was

**Table 1.** Correlation coefficient and NSE (Nash–Sutcliffe efficiency) between the EC flux and the other two methods. CT denotes Carbon-Tracker and FA denotes the flux aggregation method.

| Distance | | 5 km | 10 km | 20 km | 50 km | 100 km | 200 km | 300 km | 600 km |
|---|---|---|---|---|---|---|---|---|---|
| CT | NSE | N/A | N/A | N/A | N/A | 0.41 | 0.82 | 0.92 | 0.97 |
| | $r$ | N/A | N/A | N/A | N/A | 0.96 | 0.97 | 0.98 | 0.99 |
| FA | NSE | 0.48 | 0.49 | 0.37 | 0.23 | 0.58 | 0.90 | 0.95 | 0.96 |
| | $r$ | 0.98 | 0.98 | 0.98 | 0.98 | 0.98 | 0.98 | 0.98 | 0.98 |

$-0.09 \pm 0.02 \, \mathrm{mol \, m^{-2} \, s^{-1}}$ (mean $\pm 1$ standard deviation of the three estimates) The $CH_4$ and $N_2O$ fluxes were $16.0 \pm 3.1$ and $0.19 \pm 0.04 \, \mathrm{nmol \, m^{-2} \, s^{-1}}$, respectively.

In order to estimate an annual budget of $CH_4$ and $N_2O$ with the EQ method, we need the $CH_4$ and $N_2O$ mixing ratio within and above the boundary layer for the whole year. Therefore, we assumed that the seasonal pattern of the $CH_4$ and $N_2O$ mixing ratios at the KCMP tower was identical to the pattern at a nearby NOAA tall tower site (WBI in Iowa) (Andrews et al., 2013, 2014; Dlugokencky et al., 2013), and we extrapolated the $CH_4$ and $N_2O$ concentration during the intensive campaign period to the whole year for 2009 according to the seasonal pattern at the WBI site. The WBI site was chosen because it has similar land cover types to the KCMP tower site in its footprint (Zhang et al., 2014). The $CH_4$ and $N_2O$ mixing ratios above the boundary layer were determined at the NWR site and $\rho W$ was determined by the three methods (Eqs. 3–5) throughout the year 2009 (Fig. S6 in the Supplement). It follows that the annual regional $CH_4$ and $N_2O$ fluxes were $22.4 \pm 4.2$ and $0.49 \pm 0.09 \, \mathrm{nmol \, m^{-2} \, s^{-1}}$, respectively. The uncertainties of the annual fluxes were the result of the uncertainties in $\rho W$. In comparison, the annual $CH_4$ and $N_2O$ fluxes at the WBI tower were 14.5 and $0.32 \, \mathrm{nmol \, m^{-2} \, s^{-1}}$ using the EQ method (Zhang, 2013). The impact of advection was considered as negligible since there was no prevailing wind direction throughout the year of 2009.

## 4 Discussion

### 4.1 Annual carbon dioxide flux

Determining the annual $CO_2$ flux at the regional scale is challenging because the flux has both diurnal and seasonal cycles and the magnitude of the annual average is substantially smaller than the seasonal and diurnal variations. For example, in 2009, the tall tower's annual average EC flux was $-0.35 \, \mathrm{\mu mol \, m^{-2} \, s^{-1}}$ ($-131 \, \mathrm{g \, C–CO_2 \, m^{-2} \, yr^{-1}}$), while the seasonal variation was about $6 \, \mathrm{\mu mol \, m^{-2} \, s^{-1}}$ and the diurnal variation during summertime was about $40 \, \mathrm{\mu mol \, m^{-2} \, s^{-1}}$, about 16 and 113 times, respectively, higher than the annual average. So far, there is no single method that can directly assess the regional $CO_2$ flux because for all the available methods there are periods or conditions where the underlying the-

ory is not met or where the available data is limited to truly capture the temporal and spatial variability. A small systematic bias in the daily and monthly flux estimation, such as that caused by the data-screening and gap-filling approaches, is significant for the annual average $CO_2$ flux, and it may result in opposite conclusions of whether the landscape is a carbon source or a sink.

A number of studies have attempted to estimate the annual $CO_2$ flux in the vicinity of the upper Midwest, USA (Table 2) (Davis et al., 2003; Bakwin et al., 2004; Helliker et al., 2004; Ricciuto et al., 2008). Based on EC measurements on the LEF tall tower, which is about 260 km northeast of the KCMP tower, Ricciuto et al. (2008) reported that the annual $CO_2$ flux was $120 \, \mathrm{g \, C–CO_2 \, m^{-2} \, yr^{-1}}$, with a strong interannual variation from 1997 to 2004 ($140 \, \mathrm{g \, C–CO_2 \, m^{-2} \, yr^{-1}}$). This result was similar to the Davis et al. (2003) result, but opposite the Helliker et al. (2004) EC flux for 2000, the latter of which is $-71 \, \mathrm{g \, C–CO_2 \, m^{-2} \, yr^{-1}}$. The major difference is that Helliker et al. (2004) did not gap-fill the data, and the reported $CO_2$ flux has excluded the periods when water vapor flux was not available.

Our annual $CO_2$ flux was calculated as the average of monthly fluxes, and the monthly fluxes were determined by the diurnal composite of available observations after $u_*$ and storage term screening. We performed a Monte Carlo simulation to assess the uncertainty associated with missing data following Griffis et al. (2003). We randomly removed 30 % of the data for each month, and recorded the calculated monthly and annual fluxes following the same data processing procedure. By repeating this simulation 5000 times, we determined the standard deviation of the annual flux estimates. As a result, the uncertainty in the annual $CO_2$ flux due to data gaps was $\pm 31 \, \mathrm{g \, C \, m^{-2} \, yr^{-1}}$. In addition, the random errors in hourly averaged EC flux may also significantly affect the annual budget. Assuming a 20 % random error in hourly EC flux, the resulting uncertainties in annual flux was $\pm 4 \, \mathrm{g \, C \, m^{-2} \, yr^{-1}}$, about one magnitude lower than the uncertainties from data gaps (Morgenstern et al., 2004). Considering the uncertainties from data gaps and random errors, the 2009 $CO_2$ budget was $-131 \pm 35 \, \mathrm{g \, C \, m^{-2} \, yr^{-1}}$, suggesting the region around the tall tower was a carbon sink.

The uncertainty of the annual FA estimate was affected by the accuracy of the land cover information, the carbon flux data for each land cover type, and anthropogenic emissions.

**Table 2.** A summary of annual net ecosystem exchange estimated from different methods. Net ecosystem exchange in the Reference column is from the study in the Midwest, USA in recent years. Negative fluxes indicate carbon sink from the atmosphere and positive fluxes indicate carbon release to the atmosphere.

| | This study (g C–CO$_2$ m$^{-2}$ yr$^{-1}$) | Reference (g C–CO$_2$ m$^{-2}$ yr$^{-1}$) |
|---|---|---|
| Tall tower Eddy Covariance | $-131 \pm 35$ | $120 \pm 140$ (1997–2004) (Ricciuto et al., 2010) |
| | | $16 \pm 19$ (1997) (Davis et al., 2003) |
| | | $-71$ (2000) (Helliker et al., 2004) |
| | | $16$ (1997) (Bakwin et al., 2004) |
| CarbonTracker | $-54 \pm 12$ | $-58$ (2000–2006) (Desai et al., 2010) |
| Equilibrium | 46–74 | $-110 \pm 14$ (1997–2006) (Desai et al., 2010) |
| | | $-38$ (2000) (Helliker et al., 2004) |
| | | $79$ (1997) (Bakwin et al., 2004) |
| Flux Aggregation | $-130 \pm 34$ | |
| Corn | $-599 \pm 26$ | $-466 \pm 38$ (2004–2007) (Hernandez-Ramirez et al., 2011) |
| | | $-576 \pm 101$ (1997–2002) (Hollinger et al., 2005) |
| Soybean | $10 \pm 18$ | $-13 \pm 39$ (2004–2007) (Hernandez-Ramirez et al., 2011) |
| | | $-32 \pm 161$ (1997–2002) (Hollinger et al., 2005) |
| Grassland | $-411 \pm 10$ | $-148 \pm 116$ (1997–1999) (Suyker et al., 2003) |
| Forest | $-227 \pm 14$ | $-137 \pm 49$ (1999–2001) (Schmid et al., 2003) |
| Fossil fuel | $124 \pm 12$ | |
| Other methods | | |
| Interannual Flux Tower Upscaling Experiment | | $-321 \pm 13$ (1997–2006) (Desai et al., 2010) |
| Mesoscale inverse modeling | | $-183 \pm 35$ (1997–2006) (Lauvaux et al., 2012) |

We assessed the uncertainties of the annual CO$_2$ flux from each land cover type with the method used for tall tower EC flux (Table 2) and assume the uncertainty of anthropogenic emissions was 10 % (NRC, 2010). Without considering the uncertainties in land cover information, the annual FA flux was $-130 \pm 13$ g C m$^{-2}$ yr$^{-1}$. The accuracy of the Cropland Data Layer was 85–95 % for major crops (Boryan et al., 2011); therefore, we assume that the fraction of each land cover type has an uncertainty of up to 20 %. By using a Monte Carlo simulation we estimated that the uncertainty of the annual FA estimate will increase to 34 g C m$^{-2}$. In other words, the FA annual flux ($-130 \pm 34$ g C–CO$_2$ m$^{-2}$ yr$^{-1}$) showed very good agreement with the EC flux in 2009.

Although the CT monthly flux tracked the seasonal pattern of the EC and FA flux, the annual CT flux was $-54$ g C–CO$_2$ m$^{-2}$ yr$^{-1}$, considerably lower than EC and FA annual fluxes. This indicates that the CT method performed reasonably well on reproducing the monthly fluxes, but that it systematically underestimated the annual flux compared to the other methods.

Overall, the good agreement between the EC (a top-down method) and FA (a bottom-up method) provides strong evidence that the landscape around the tall tower was a carbon sink, at the rate of $-131 \pm 35$ g C m$^{-2}$ yr$^{-1}$ in 2009.

## 4.2 Uncertainties in CO$_2$ flux from the equilibrium method

The EQ method provided good estimates of the CO$_2$ flux for each month except July, when the regional CO$_2$ flux was the most negative (strong sink) during 2009. Excluding July, the difference between the monthly EC flux and EQ flux in 2009 was $0.37 \pm 0.29 \,\mu\text{mol m}^{-2}\,\text{s}^{-1}$, only 6 % of the seasonal variation ($6 \,\mu\text{mol m}^{-2}\,\text{s}^{-1}$).

The underestimation of the EQ flux might be attributed to uncertainties in $\rho W$ or concentration differences at the top of boundary layer ($c_+ - c_m$), according to Eq. (2). In July, the $\rho W$ was $-0.17 \,\text{mol m}^{-2}\,\text{s}^{-1}$ (Eq. 3) and $-0.26 \,\text{mol m}^{-2}\,\text{s}^{-1}$ (Eq. 4) while the concentration difference was 9.03 ppm. To bring the equilibrium flux into agreement with the tall-tower EC flux ($-4.82 \,\mu\text{mol m}^{-2}\,\text{s}^{-1}$ in July 2009), $\rho W$ would have to increase to $-0.53 \,\text{mol m}^{-2}\,\text{s}^{-1}$, which is much larger in magnitude than $-0.26 \pm 0.09 \,\text{mol m}^{-2}\,\text{s}^{-1}$, the average July value for 2007 to 2011 obtained with the NCEP reanalysis data. The 0.09 mol m$^{-2}$ s$^{-1}$ uncertainty in $\rho W$ (the standard deviation of July $\rho W$ from 2007 to 2011) leads to $0.81 \,\mu\text{mol m}^{-2}\,\text{s}^{-1}$ uncertainty in the monthly flux, about 17 % of the July flux. In addition, the monthly $\rho W$ values in 2007 to 2011 period were mostly within $-0.18 \pm 0.08 \,\text{mol m}^{-2}\,\text{s}^{-1}$, and the maximum and minimum values were $-0.05$ and $-0.36 \,\text{mol m}^{-2}\,\text{s}^{-1}$. Even the most negative value in the 5-year period cannot fully explain the underestimation of the EQ flux in July, indicating that the

concentration differences at the top of boundary layer may be underestimated.

Two sources of uncertainty exist in the concentration difference observed at the top of boundary layer ($c_+ - c_m$). One is the accuracy of the $CO_2$ measurement at 200 m level of the KCMP tower site and NWR background site, and the other is the assumption that those two concentrations are the same as the concentration within and above the boundary layer. The $CO_2$ concentration at the KCMP tower was calibrated with the NOAA-ESRL standard throughout the measurement, and the measurement precision was 0.03 ppm. Meanwhile, the precision at the NWR site was on the order of 0.1 ppm (Helliker et al., 2004). As a result the first source of uncertainty led to about 0.04 $\mu$mol m$^{-2}$ s$^{-1}$ uncertainties, which was not significant.

The second source of uncertainty can potentially lead to 1.55 $\mu$mol m$^{-2}$ s$^{-1}$ uncertainties in the July $CO_2$ flux. Even though the NWR site is only about 5° south of the KCMP tower, the $CO_2$ concentration at the NWR site may be significantly different from the $CO_2$ concentration above the boundary layer at the KCMP site, due to a large latitudinal $CO_2$ gradient (Denning et al., 1995). To examine the uncertainties in using the $CO_2$ concentration at the NWR site as a proxy for $c_+$ we surveyed the following observation data that could be used as a proxy for $c_+$ in July 2009: (1) the $CO_2$ concentration in the marine boundary layer at the same latitude as the KCMP tower was 382.47 ppm; (2) the average $CO_2$ concentration measured by aircraft (between 3000–4500 m) at three sites near the KCMP tower was 384.80 ± 4.55 ppm (Cooperative Global Atmospheric Data Integration Project, 2014; Yi et al., 2004); (3) the average $CO_2$ concentrations in the nearby background sites were 380.03 ppm (Cold Bay, Alaska, USA) and 383.81 ppm (Barrow, Alaska, USA). The $CO_2$ concentration at the NWR site (386.01 ppm) is not significantly different from the aircraft measurements and is lower than the rest of the concentrations, with the maximum difference of 5.98 ppm. Therefore, the $CO_2$ concentration at NWR site may overestimate $c_+$ by up to 5.98 ppm and result in up to 1.55 $\mu$mol m$^{-2}$ s$^{-1}$ of uncertainty in the July $CO_2$ flux. The uncertainties in other months in 2009 were examined and are presented in the Supplement (Sect. S4).

Bakwin et al. (2004) adjusted the $CO_2$ concentration at the 30 m height by increasing it by 2.5 ppm to estimate $c_m$ in the summer. Since our $CO_2$ concentration was measured at 200 m, a much higher level, the uncertainty in using 200 m concentration to estimate $c_m$ should be much less than 2.5 ppm. Direct measurement at the top of the boundary layer is needed to evaluate these two important uncertainties.

Another more likely source for the significant underestimation in July is that horizontal advection is not negligible when the prevailing winds align with a strong spatial $CO_2$ gradient. With a tall tower observation network, Miles et al. (2012) reported that the $CO_2$ gradients between the KCMP tower and other sites range from 0.3 to
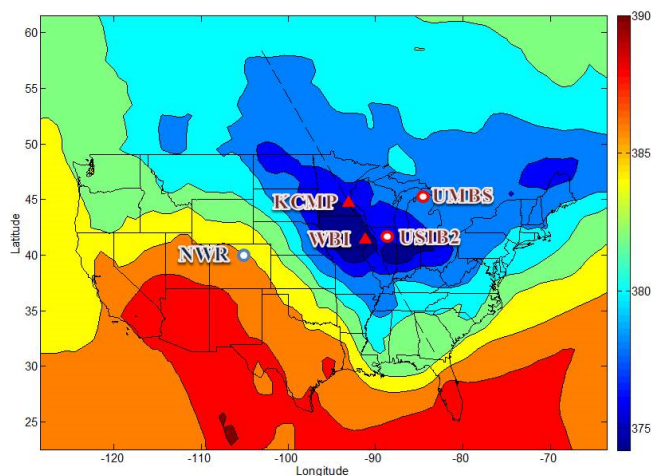


**Figure 5.** $CO_2$ concentration averaged from land surface to 1274.1 m according to the CarbonTracker 3-D $CO_2$ concentration product in July, 2009. Dashed line – prevailing wind direction in July from northwest to southeast. Red triangle – the KCMP tower site and WBI tower observatory operated by NOAA. Red circle – Ameriflux sites. Blue circle – background observation site. The color scale is the $CO_2$ concentration in ppm. The resolution of the concentration data is 1° by 1°.

2.1 ppm 100 km$^{-1}$ during the growing season. The CarbonTracker 3-D $CO_2$ concentration product also shows large $CO_2$ depletion in the upper Midwest Corn Belt during the growing season due to the strong $CO_2$ uptake by corn plants. According to this product, the mean concentration of the 34–1274 m air layer has an averaged gradient of 0.8 ppm 100 km$^{-1}$ along the prevailing wind (from northwest) in July 2009 (Fig. 5). Using a mean wind speed of 5.4 m s$^{-1}$ recorded on the tall tower and a boundary layer depth of 1000 m (Yi et al., 2001), the resulting advection flux was −1.88 $\mu$mol m$^{-2}$ s$^{-1}$, which is comparable to the bias of the equilibrium method. In comparison, the EC flux was not as sensitive to the advective influence. For instance, using the same spatial gradient data, the advection flux at the 100 m level was only −0.02 $\mu$mol m$^{-2}$ s$^{-1}$ according to the accumulated concentration for the lowest two grid levels in the CarbonTracker product (34.5 and 112 m).

Overall, the uncertainties in $\rho W$, $c_+ - c_m$, and horizontal advection can potentially lead to uncertainties in the July $CO_2$ flux estimates on the order of 0.81, 1.55, and −1.88 $\mu$mol m$^{-2}$ s$^{-1}$, respectively, and they might be large enough to account for the discrepancy between EQ and EC methods for July 2009 and the annual 2009 flux. Direct and accurate measurements of these three terms using methods such as drones or other aircraft (Yi et al., 2004) are needed to reduce these uncertainties.

### 4.3 Uncertainties in the $CH_4$ and $N_2O$ fluxes

Uncertainties in trace gas concentration measurements within and above the boundary layer can lead to large uncertainties in the trace gas flux estimation. The averaged $CH_4$ concentrations during the intensive campaign at the nearby background sites were 1.883 ppm (Cold Bay, Alaska, USA), 1.887 ppm (Barrow, Alaska, USA), and 1.842 ppm (NWR, Colorado, USA). The maximum difference between NWR and the other background sites in North America was 0.045 ppm. If the measurements at these other sites were used for the concentration above the boundary layer at the tall tower site, the regional flux would decrease by up to 4.1 nmol m$^{-2}$ s$^{-1}$, or about 30 % of the estimated EQ flux. In addition, the uncertainty in our $CH_4$ concentration measurement caused by uncertainties in the calibration standard was 0.055 ppm, with a resulting uncertainty in the flux of $\pm 5.0$ nmol m$^{-2}$ s$^{-1}$. The combined uncertainty range of the $CH_4$ flux is 6.9–21.0 nmol m$^{-2}$ s$^{-1}$.

The systematic bias in the trace gas measurement between the KCMP tower and NOAA background sites was avoided in the other two independent boundary layer methods, which depend on the relative concentration differences at 3 and 200 m levels and the concentration build-up (change in concentration with time) at night. Here, we used these two methods, a modified Bowen ratio method (Werner et al., 2003) and a modified nocturnal boundary layer method (Kelliher et al., 2002), to calculate the nighttime $CH_4$ flux for comparison with the equilibrium estimate. The modified Bowen ratio method assumes that the vertical transport of a trace gas is driven by eddy diffusion and that the diffusivity is the same for all scalar quantities. The nocturnal boundary layer method uses $CO_2$ as a tracer and assumes that the build-up of $CO_2$ and $CH_4$ near the land surface is caused by land surface emissions. The $CH_4$ fluxes from these two methods were $14.8 \pm 10.3$ and $17.1 \pm 9.4$ nmol m$^{-2}$ s$^{-1}$ (Zhang et al., 2013), respectively. The results confirm that the $CH_4$ flux from the equilibrium method (16.0 nmol m$^{-2}$ s$^{-1}$) gave a reasonable estimation of the regional flux.

$N_2O$ has a much more homogeneous background concentration than $CH_4$ and $CO_2$. The differences between the background sites in the Northern Hemisphere were less than 0.5 ppb during the intensive campaign. The $N_2O$ measurements at the tall tower were calibrated against NOAA-ESRL standards and, therefore, can be compared against the NOAA background sites. The uncertainties in the background concentration will lead to a bias within 0.05 nmol m$^{-2}$ s$^{-1}$ for the $N_2O$ flux estimation, or 26 % of the estimated $N_2O$ flux (0.19 nmol m$^{-2}$ s$^{-1}$). Applying the modified Bowen ratio method and the modified nocturnal boundary layer method, we obtained a regional nighttime $N_2O$ flux of $1.09 \pm 0.56$ and $0.90 \pm 0.65$ nmol m$^{-2}$ s$^{-1}$, respectively, both of which were higher than the flux estimated from the equilibrium method. It is possible that EQ method underestimated the regional $N_2O$ flux because the advection was not negligible during the

intensive observation period, but it is not feasible to evaluate due to scarce $N_2O$ concentration measurements.

### 4.4 Climate impact of the major GHG fluxes

According to the KCMP tower measurement, the regional fluxes of three major greenhouse gases in 2009 were $-131 \pm 35$ g C–$CO_2$ m$^{-2}$ yr$^{-1}$, $8.50 \pm 1.58$ g C–$CH_4$ m$^{-2}$ yr$^{-1}$, and $0.43 \pm 0.08$ N–$N_2O$ m$^{-2}$ yr$^{-1}$. The global warming potential (GWP) over a 100-year time horizon for $CO_2$, $CH_4$, and $N_2O$ was $-480 \pm 128$, $283 \pm 53$, and $205 \pm 37$ g $CO_2$ equivalent m$^{-2}$ yr$^{-1}$, respectively. The GWP for $CO_2$ was a result of anthropogenic emissions (454 g $CO_2$ equivalent m$^{-2}$ yr$^{-1}$, according to the fossil fuel emissions prescribed in the CarbonTracker product) and biological $CO_2$ uptake (934 g $CO_2$ equivalent m$^{-2}$ yr$^{-1}$) for the region around the tall tower (Table 2). The total climate impact of the $CH_4$ and $N_2O$ emissions offset about 30 and 22 % of the biological $CO_2$ uptake and was comparable to the anthropogenic $CO_2$ emission, indicating the important role of $CH_4$ and $N_2O$ for the regional GHG emission portfolio.

Considering all three major GHG fluxes, the landscape around the tall tower had a near neutral impact on the climate in 2009 ($7 \pm 160$ g $CO_2$ equivalent m$^{-2}$ yr$^{-1}$). This conclusion, however, did not consider that the carbon fixed by crops will be harvested and some fraction will be transported and emitted outside of the tall tower footprint. According to West et al. (2011), the harvested biomass from the KCMP tower footprint is approximately 140 g C m$^{-2}$ yr$^{-1}$ (513 g $CO_2$ equivalent m$^{-2}$ yr$^{-1}$). In other words, the tall tower footprint likely has a warming impact on the climate when all three major GHG fluxes and emission leakage (i.e., loss of carbon to the atmosphere from harvested biomass) are considered.

### 4.5 Comparison with bottom-up inventories

EDGAR is a widely used anthropogenic GHG inventory for atmospheric research, with fine spatial resolution ($0.1° \times 0.1°$) (Jeong et al., 2012; Zhao et al., 2009). So far, only a few studies have evaluated it with atmospheric observations. These studies indicate that EDGAR may have significantly underestimated $N_2O$ and $CH_4$ emissions in North America by a factor of 3 (Kort et al., 2008; Miller et al., 2012).

We first compared the $CH_4$ and $N_2O$ fluxes at the KCMP tower during the intensive campaign with EDGAR42 for the area within the 300 km radius around the tower, and found that the $CH_4$ flux was 5.8 times higher and the $N_2O$ flux was 50 % higher than the EDGAR42 values. In this comparison, the EDGAR42 annual estimate was scaled to the emissions in September using its seasonal factor (1.1 for September). Another comparison was carried out on the annual timescale. The estimates of the annual $CH_4$ and $N_2O$ fluxes based on the tall tower EQ measurement were 6–9 times and 2–3 times higher than the EDGAR42 annual flux, respectively.

The primary reason for the lower regional $CH_4$ flux from EDGAR42 is because it excludes natural sources of $CH_4$. Wetlands are the major natural $CH_4$ source in this region. Although wetlands account for less than 5 % of the land around the tall tower, it is not negligible in the regional $CH_4$ budgeting because $CH_4$ emissions from wetlands can be as high as $250\,nmol\,m^{-2}\,s^{-1}$ in September (Bridgham et al., 2006). EDGAR42 may have also underestimated the $CH_4$ emissions from anthropogenic sources because it does not account for factors such as natural gas leakage, and has low biases for the $CH_4$ emissions from agricultural activities (Mays et al., 2009; Wunch et al., 2009; Ussiri et al., 2009).

We hypothesize that the lower $N_2O$ flux in the EDGAR42 inventory is likely a result of the underestimation of anthropogenic $N_2O$ emission, since natural sources were not significant in the region around the tall tower. A recent study on global $N_2O$ emissions from a natural ecosystems suggests soil emissions in the upper Midwest, USA is mostly around $0.10\,kg\,N\,ha^{-1}\,yr^{-1}$ ($0.01\,nmol\,m^{-2}\,s^{-1}$) (Zhuang et al., 2012), only 10 % of the EDGAR42 anthropogenic emission.

In addition to EDGAR42, we compare the $CH_4$ and $N_2O$ fluxes measured at the KCMP tower with the GHG inventory developed by the EPA (EPA inventory), which was based on more country-specific emission factors or models (e.g., $N_2O$ from agriculture soil was simulated with a biogeochemical model). The national $CH_4$ and $N_2O$ emissions in the EPA inventory were 12 and 35 % higher than in the EDGAR42 inventory. However, we cannot directly compare the EPA inventory with the top-down estimates for a region since the EPA inventory does not have a spatial distribution for all emission sectors. If we assume that the spatial distribution of the EPA inventory is the same as the EDGAR42 inventory, the EPA inventory brings the bottom-up estimates closer to the top-down EQ estimates. But the tall tower EQ estimates for regional $CH_4$ and $N_2O$ emissions were still 5–8 times and 1–2 times higher than the EPA inventory.

## 5   Conclusions

The regional budget of $CO_2$, $CH_4$, and $N_2O$ for the upper Midwest, USA was quantified with multiple top-down and bottom-up approaches. The four methods for the regional $CO_2$ flux (tall-tower eddy covariance, CarbonTracker inverse modeling, flux aggregation, and the equilibrium boundary layer method) produced similar seasonal patterns (linear correlation of the monthly flux $> 0.85$, $p < 0.001$). However, discrepancies exist in the magnitude of the monthly and annual fluxes. The CarbonTracker annual flux for 2009 ($-54\,g\,C$–$CO_2\,m^{-2}\,yr^{-1}$) was much lower in magnitude than the flux aggregation estimate ($-130 \pm 37\,g\,C$–$CO_2\,m^{-2}\,yr^{-1}$) and that measured with eddy covariance ($-131 \pm 40\,g\,C$–$CO_2\,m^{-2}\,yr^{-1}$). The equilibrium method significantly underestimated the July uptake by 52–69 % in comparison to eddy covariance. The underestimation cannot be fully explained by the bias in $\rho W$ or concentration differences at the top of the boundary layer, and we suggest that the large spatial gradient along the prevailing wind in July 2009 was a main contributor to the underestimation.

The $CH_4$ and $N_2O$ regional fluxes estimated from the equilibrium method during the intensive campaign (DOY 243 – 269, 2009) were $16.0 \pm 3.1$ and $0.19 \pm 0.04\,nmol\,m^{-2}\,s^{-1}$, respectively, and were 5.8 times and 50 % higher than in the EDGAR42 inventory. The annual $CH_4$ and $N_2O$ fluxes also suggest significant underestimation by the EDGAR42 inventory and the EPA inventory.

Considering the global warming potential on a 100-year timescale, the $CH_4$ and $N_2O$ emissions from the landscape were comparable to the anthropogenic $CO_2$. The landscape appeared to have a near-neutral impact on climate when all three major GHGs were considered. Our results confirm that for this agriculture-dominated landscape, climate change mitigation should include $CH_4$ and $N_2O$ emissions.

**The Supplement related to this article is available online at doi:10.5194/acp-14-10705-2014-supplement.**

## References

Andrews, A. E., Lang, P. M., Crotwell, A. J., and Kofler, J. D.: Nitrous Oxide Dry Air Mole Fractions from the NOAA ESRL Tall Tower Network using Programmable Flask Packages (PFP), Version: 2012-09-21, 2013.

Andrews, A. E., Kofler, J. D., Trudeau, M. E., Williams, J. C., Neff, D. H., Masarie, K. A., Chao, D. Y., Kitzis, D. R., Novelli, P. C., Zhao, C. L., Dlugokencky, E. J., Lang, P. M., Crotwell, M. J., Fischer, M. L., Parker, M. J., Lee, J. T., Baumann, D. D., Desai, A. R., Stanier, C. O., De Wekker, S. F. J., Wolfe, D. E., Munger, J. W., and Tans, P. P.: $CO_2$, CO, and $CH_4$ measurements from tall towers in the NOAA Earth System Research

Laboratory's Global Greenhouse Gas Reference Network: instrumentation, uncertainty analysis, and recommendations for future high-accuracy greenhouse gas monitoring efforts, Atmos. Meas. Tech., 7, 647–687, doi:10.5194/amt-7-647-2014, 2014.

Anthoni, P. M., Law, B. E., and Unsworth, M. H.: Carbon and water vapor exchange of an open-canopied ponderosa pine ecosystem, Agric. For. Meteorol., 95, 151–168, doi:10.1016/s0168-1923(99)00029-5, 1999.

Baker, J. M. and Griffis, T. J.: Examining strategies to improve the carbon balance of corn/soybean agriculture using eddy covariance and mass balance techniques, Agric. For. Meteorol., 128, 163–177, doi:10.1016/j.agrformet.2004.11.005, 2005.

Bakwin, P. S., Davis, K. J., Yi, C., Wofsy, S. C., Munger, J. W., Haszpra, L., and Barcza, Z.: Regional carbon dioxide fluxes from mixing ratio data, Tellus B, 56, 301–311, doi:10.1111/j.1600-0889.2004.00111.x, 2004.

Betts, A. K.: Idealized model for equilibrium boundary layer over land, J. Hydrometeorol., 1, 507–523, doi:10.1175/1525-7541(2000)001<0507:Imfebl>2.0.Co;2, 2000.

Betts, A. K., Helliker, B., and Berry, J.: Coupling between $CO_2$, water vapor, temperature, and radon and their fluxes in an idealized equilibrium boundary layer over land, J. Geophys. Res.-Atmos., 109, D18103, doi:10.1029/2003jd004420, 2004.

Boden, T. A., Marland, G., and Andres, R. J.: Global, Regional, and National Fossil-Fuel $CO_2$ Emissions, Carbon Dioxide Information Analysis Center, Oak Ridge National Laboratory, US Department of Energy, Oak Ridge, Tenn., USA, doi:10.3334/CDIAC/00001_V2011, 2011.

Boryan, C., Yang, Z. W., Mueller, R., and Craig, M.: Monitoring US agriculture: the US Department of Agriculture, National Agricultural Statistics Service, Cropland Data Layer Program, Geocarto Int., 26, 341–358, doi:10.1080/10106049.2011.562309, 2011.

Bridgham, S. D., Megonigal, J. P., Keller, J. K., Bliss, N. B., and Trettin, C.: The carbon balance of North American wetlands, Wetlands, 26, 889–916, doi:10.1672/0277-5212(2006)26[889:Tcbona]2.0.Co;2, 2006.

Chen, B., Chen, J. M., Mo, G., Black, A., and Worthy, D. E. J.: Comparison of regional carbon flux estimates from $CO_2$ concentration measurements and remote sensing based footprint integration, Global Biogeochem. Cy., 22, GB2012, doi:10.1029/2007gb003024, 2008.

Chen, B. Z., Black, T. A., Coops, N. C., Hilker, T., Trofymow, J. A., and Morgenstern, K.: Assessing Tower Flux Footprint Climatology and Scaling Between Remotely Sensed and Eddy Covariance Measurements, Bound-Lay. Meteorol., 130, 137–167, 2009.

Conway, T. J., Tans, P. P., Waterman, L. S., and Thoning, K. W.: Evidence for Interannual Variability of the Carbon-Cycle from the National-Oceanic-and-Atmospheric-Administration Climate-Monitoring-and-Diagnostics-Laboratory Global-Air-Sampling-Network, J. Geophys. Res.-Atmos., 99, 22831–22855, doi:10.1029/94jd01951, 1994.

Cooperative Global Atmospheric Data Integration Project: Multi- laboratory compilation of atmospheric carbon dioxide data for the period 2000–2013 (obspack_co2_1_CARBONTRACKER_CT2013_2014-05-08), Compiled by NOAA Global Monitoring Division: Boulder, Colorado, USA Data product accessed at http://www.esrl.noaa.gov/gmd/ccgg/obspack/, last access: 3 July 2014.

Curtis, P. S., Vogel, C. S., Gough, C. M., Schmid, H. P., Su, H. B., and Bovard, B. D.: Respiratory carbon losses and the carbon-use efficiency of a northern hardwood forest, 1999–2003, New Phytol., 167, 437–455, doi:10.1111/j.1469-8137.2005.01438.x, 2005.

Davis, K. J., Bakwin, P. S., Yi, C. X., Berger, B. W., Zhao, C. L., Teclaw, R. M., and Isebrands, J. G.: The annual cycles of $CO_2$ and $H_2O$ exchange over a northern mixed forest as observed from a very tall tower, Global Change Biol., 9, 1278–1293, doi:10.1046/j.1365-2486.2003.00672.x, 2003.

Denmead, O. T., Raupach, M. R., Dunin, F. X., Cleugh, H. A., and Leuning, R.: Boundary layer budgets for regional estimates of scalar fluxes, Global Change Biol., 2, 255–264, doi:10.1111/j.1365-2486.1996.tb00077.x, 1996.

Denning, A. S., Fung, I. Y., and Randall, D. A.: Latitudinal gradient of atmospheric $CO_2$ due to seasonal exchange with land biota, Nature, 376, 240–243, 1995.

Desai, A. R.: Climatic and phenological controls on coherent regional interannual variability of carbon dioxide flux in a heterogeneous landscape, J. Geophys. Res.-Biogeo., 115, G00J02, doi:10.1029/2010jg001423, 2010.

Desai, A. R., Noormets, A., Bolstad, P. V., Chen, J. Q., Cook, B. D., Davis, K. J., Euskirchen, E. S., Gough, C. M., Martin, J. G., Ricciuto, D. M., Schmid, H. P., Tang, J. W., and Wang, W. G.: Influence of vegetation and seasonal forcing on carbon dioxide fluxes across the Upper Midwest, USA: Implications for regional scaling, Agric. For. Meteorol., 148, 288–308, doi:10.1016/j.agrformet.2007.08.001, 2008.

Desai, A. R., Helliker, B. R., Moorcroft, P. R., Andrews, A. E., and Berry, J. A.: Climatic controls of interannual variability in regional carbon fluxes from top-down and bottom-up perspectives, J. Geophys. Res.-Biogeo., 115, G02011, doi:10.1029/2009jg001122, 2010.

Desai, A. R., Wang, W. G., and Cook, B. D.: Uncovering mechanisms of episodic methane sources observed by a very tall eddy covariance tower, 30th Conference on Agric. For. Meteorol./1st Conference on Atmospheric Biogeosciences, Boston, MA, US, 2012.

Dlugokencky, E., Lang, P. M., and Crotwell, A. J.: Nitrous Oxide Dry Air Mole Fractions from the NOAA ESRL Global Cooperative Air Sampling Network, Version: 2012-09-21, 2013.

Gash, J. H. C.: A Note on Estimating the Effect of a Limited Fetch on Micrometeorological Evaporation Measurements, Bound.-Lay. Meteorol., 35, 409–413, doi:10.1007/Bf00118567, 1986.

Gloor, M., Bakwin, P., Hurst, D., Lock, L., Draxler, R., and Tans, P.: What is the concentration footprint of a tall tower?, J. Geophys. Res-Atmos., 106, 17831–17840, doi:10.1029/2001jd900021, 2001.

Gomez-Casanovas, N., Matamala, R., Cook, D. R., and Gonzalez-Meler, M. A.: Net ecosystem exchange modifies the relationship between the autotrophic and heterotrophic components of soil respiration with abiotic factors in prairie grasslands, Global Change Biol., 18, 2532–2545, doi:10.1111/J.1365-2486.2012.02721.X, 2012.

Goulden, M. L., Munger, J. W., Fan, S. M., Daube, B. C., and Wofsy, S. C.: Measurements of carbon sequestration by long-term eddy covariance: Methods and a critical evaluation of accuracy, Global Change Biol., 2, 169–182, doi:10.1111/j.1365-2486.1996.tb00070.x, 1996.

Griffis, T. J., Black, T. A., Morgenstern, K., Barr, A. G., Nesic, Z., Drewitt, G. B., Gaumont-Guay, D., and McCaughey, J. H.: Ecophysiological controls on the carbon balances of three southern boreal forests, Agric. For. Meteorol., 117, 53–71, doi:10.1016/s0168-1923(03)00023-6, 2003.

Griffis, T. J., Lee, X., Baker, J. M., Sargent, S. D., and King, J. Y.: Feasibility of quantifying ecosystem-atmosphere $C^{18}O^{16}O$ exchange using laser spectroscopy and the flux-gradient method, Agric. For. Meteorol., 135, 44–60, doi:10.1016/j.agrformet.2005.10.002, 2005.

Griffis, T. J., Baker, J. M., Sargent, S. D., Erickson, M., Corcoran, J., Chen, M., and Billmark, K.: Influence of $C_4$ vegetation on $^{13}CO_2$ discrimination and isoforcing in the upper Midwest, United States, Global Biogeochem. Cy., 24, GB4006, doi:10.1029/2009gb003768, 2010.

Griffis, T. J., Lee, X., Baker, J. M., Russelle, M. P., Zhang, X., Venterea, R., and Millet, D. B.: Reconciling the differences between top-down and bottom-up estimates of nitrous oxide emissions for the US Corn Belt, Global Biogeochem. Cy., 27, 746–754, doi:10.1002/gbc.20066, 2013.

Haszpra, L., Barcza, Z., Davis, K. J., and Tarczay, K.: Long-term tall tower carbon dioxide flux monitoring over an area of mixed vegetation, Agric. For. Meteorol., 132, 58–77, doi:10.1016/j.agrformet.2005.07.002, 2005.

Helliker, B. R., Berry, J. A., Betts, A. K., Bakwin, P. S., Davis, K. J., Denning, A. S., Ehleringer, J. R., Miller, J. B., Butler, M. P., and Ricciuto, D. M.: Estimates of net $CO_2$ flux by application of equilibrium boundary layer concepts to $CO_2$ and water vapor measurements from a tall tower, J. Geophys. Res.-Atmos., 109, D20106, doi:10.1029/2004jd004532, 2004.

Hernandez-Ramirez, G., Hatfield, J. L., Parkin, T. B., Sauer, T. J., and Prueger, J. H.: Carbon dioxide fluxes in corn-soybean rotation in the midwestern US: Inter- and intra-annual variations, and biophysical controls, Agric. For. Meteorol., 151, 1831–1842, doi:10.1016/j.agrformet.2011.07.017, 2011.

Hollinger, S. E., Bernacchi, C. J., and Meyers, T. P.: Carbon budget of mature no-till ecosystem in North Central Region of the United States, Agric. For. Meteorol., 130, 59–69, doi:10.1016/j.agrformet.2005.01.005, 2005.

Horst, T. W. and Weil, J. C.: Footprint Estimation for Scalar Flux Measurements in the Atmospheric Surface-Layer, Bound.-Lay. Meteorol., 59, 279–296, doi:10.1007/Bf00119817, 1992.

IPCC: 2006 IPCC Guidelines for National Greenhouse Gas Inventories, IGES, Japan, 2006.

Jeong, S., Zhao, C., Andrews, A. E., Bianco, L., Wilczak, J. M., and Fischer, M. L.: Seasonal variation of $CH_4$ emissions from central California, J. Geophys. Res.-Atmos., 117, D11306, doi:10.1029/2011jd016896, 2012.

Kelliher, F. M., Reisinger, A. R., Martin, R. J., Harvey, M. J., Price, S. J., and Sherlock, R. R.: Measuring nitrous oxide emission rate from grazed pasture using Fourier-transform infrared spectroscopy in the nocturnal boundary layer, Agric. For. Meteorol., 111, 29–38, doi:10.1016/S0168-1923(02)00007-2, 2002.

Kljun, N., Calanca, P., Rotach, M., and Schmid, H.: A simple parameterisation for flux footprint predictions, Bound.-Lay. Meteorol., 112, 503–523, 2004.

Knoll, L. B., Vanni, M. J., Renwick, W. H., Dittman, E. K., and Gephart, J. A.: Temperate reservoirs are large carbon sinks and small $CO_2$ sources: Results from high-resolution carbon budgets, Global Biogeochem. Cy., 27, 52–64, doi:10.1002/Gbc.20020, 2013.

Kort, E. A., Eluszkiewicz, J., Stephens, B. B., Miller, J. B., Gerbig, C., Nehrkorn, T., Daube, B. C., Kaplan, J. O., Houweling, S., and Wofsy, S. C.: Emissions of $CH_4$ and $N_2O$ over the United States and Canada based on a receptor-oriented modeling framework and COBRA-NA atmospheric observations, Geophys. Res. Lett., 35, L18808, doi:10.1029/2008gl034031, 2008.

Kroon, P. S., Hensen, A., Jonker, H. J. J., Ouwersloot, H. G., Vermeulen, A. T., and Bosveld, F. C.: Uncertainties in eddy covariance flux measurements assessed from $CH_4$ and $N_2O$ observations, Agric. For. Meteorol., 150, 806–816, 2010.

Lauvaux, T., Schuh, A. E., Uliasz, M., Richardson, S., Miles, N., Andrews, A. E., Sweeney, C., Diaz, L. I., Martins, D., Shepson, P. B., and Davis, K. J.: Constraining the $CO_2$ budget of the corn belt: exploring uncertainties from the assumptions in a mesoscale inverse system, Atmos. Chem. Phys., 12, 337–354, doi:10.5194/acp-12-337-2012, 2012.

Leclerc, M. Y. and Thurtell, G. W.: Footprint Prediction of Scalar Fluxes Using a Markovian Analysis, Bound.-Lay. Meteorol., 52, 247–258, doi:10.1007/Bf00122089, 1990.

Lee, X. H., Massman, W., and Law, B.: Handbook of Micrometeorology: A Guide for Surface Flux Measurement and Analysis, Kluwer Acad., Norwell, Mass, 250 pp., 2004.

Levy, P. E., Grelle, A., Lindroth, A., Molder, M., Jarvis, P. G., Kruijt, B., and Moncrieff, J. B.: Regional-scale $CO_2$ fluxes over central Sweden by a boundary layer budget method, Agric. For. Meteorol., 98–99, 169–180, doi:10.1016/S0168-1923(99)00096-9, 1999.

Lin, J. C., Gerbig, C., Wofsy, S. C., Andrews, A. E., Daube, B. C., Davis, K. J., and Grainger, C. A.: A near-field tool for simulating the upstream influence of atmospheric observations: The Stochastic Time-Inverted Lagrangian Transport (STILT) model, J. Geophys. Res.-Atmos., 108, 4493, doi:10.1029/2002jd003161, 2003.

Massman, W. J.: A simple method for estimating frequency response corrections for eddy covariance systems, Agric. For. Meteorol., 104, 185–198, doi:10.1016/s0168-1923(00)00164-7, 2000.

Mays, K. L., Shepson, P. B., Stirm, B. H., Karion, A., Sweeney, C., and Gurney, K. R.: Aircraft-Based Measurements of the Carbon Footprint of Indianapolis, Environ. Sci. Technol., 43, 7816–7823, doi:10.1021/Es901326b, 2009.

Miles, N. L., Richardson, S. J., Davis, K. J., Lauvaux, T., Andrews, A. E., West, T. O., Bandaru, V., and Crosson, E. R.: Large amplitude spatial and temporal gradients in atmospheric boundary layer $CO_2$ mole fractions detected with a tower-based network in the US upper Midwest, J. Geophys. Res.-Biogeo., 117, G01019, doi:10.1029/2011jg001781, 2012.

Miller, S. M., Kort, E. A., Hirsch, A. I., Dlugokencky, E. J., Andrews, A. E., Xu, X., Tian, H., Nehrkorn, T., Eluszkiewicz, J., Michalak, A. M., and Wofsy, S. C.: Regional sources of nitrous oxide over the United States: Seasonal variation and spatial distribution, J. Geophys. Res.-Atmos., 117, D06310, 2012.

Morgenstern, K., Black, T. A., Humphreys, E. R., Griffis, T. J., Drewitt, G. B., Cai, T. B., Nesic, Z., Spittlehouse, D. L., and Livingstone, N. J.: Sensitivity and uncertainty of the carbon balance of a Pacific Northwest Douglas-fir forest during an

El Nino La Nina cycle, Agric. For. Meteorol., 123, 201–219, doi:10.1016/j.agrformet.2003.12.003, 2004.

Moriasi, D. N., Arnold, J. G., Van Liew, M. W., Bingner, R. L., Harmel, R. D., and Veith, T. L.: Model evaluation guidelines for systematic quantification of accuracy in watershed simulations, T. ASABE, 50, 885–900, 2007.

Nash, J. E. and Sutcliffe, J. V.: River flow forecasting through conceptual models part I — A discussion of principles, J. Hydrol., 10, 282–290, doi:10.1016/0022-1694(70)90255-6, 1970.

National Research Council: Verifying Greenhouse Gas Emissions: Methods to Support International Climate Agreements, The National Academies Press, Washington, DC, 110 pp., 2010.

Nisbet, E. and Weiss, R.: Top-Down Versus Bottom-Up, Science, 328, 1241–1243, doi:10.1126/science.1189936, 2010.

Oda, T. and Maksyutov, S.: A very high-resolution (1 km × 1 km) global fossil fuel $CO_2$ emission inventory derived using a point source database and satellite observations of nighttime lights, Atmos. Chem. Phys., 11, 543–556, doi:10.5194/acp-11-543-2011, 2011.

Olson, D. M., Griffis, T. J., Noormets, A., Kolka, R., and Chen, J.: Interannual, seasonal, and retrospective analysis of the methane and carbon dioxide budgets of a temperate peatland, J. Geophys. Res.-Biogeo., 118, 226–238, doi:10.1002/Jgrg.20031, 2013.

Peters, W., Jacobson, A. R., Sweeney, C., Andrews, A. E., Conway, T. J., Masarie, K., Miller, J. B., Bruhwiler, L. M. P., Petron, G., Hirsch, A. I., Worthy, D. E. J., van der Werf, G. R., Randerson, J. T., Wennberg, P. O., Krol, M. C., and Tans, P. P.: An atmospheric perspective on North American carbon dioxide exchange: CarbonTracker, P. Natl. Acad. Sci. USA, 104, 18925–18930, doi:10.1073/pnas.0708986104, 2007.

Ricciuto, D. M., Butler, M. P., Davis, K. J., Cook, B. D., Bakwin, P. S., Andrews, A., and Teclaw, R. M.: Causes of interannual variability in ecosystem-atmosphere $CO_2$ exchange in a northern Wisconsin forest using a Bayesian model calibration, Agric. For. Meteorol., 148, 309–327, doi:10.1016/j.agrformet.2007.08.007, 2008.

Schmid, H. P., Su, H. B., Vogel, C. S., and Curtis, P. S.: Ecosystem-atmosphere exchange of carbon dioxide over a mixed hardwood forest in northern lower Michigan, J. Geophys. Res.-Atmos., 108, 4417, doi:10.1029/2002jd003011, 2003.

Striegl, R. G. and Michmerhuizen, C. M.: Hydrologic influence on methane and carbon dioxide dynamics at two north-central Minnesota lakes, Limnol. Oceanogr., 43, 1519–1529, 1998.

Suyker, A. E., Verma, S. B., and Burba, G. G.: Interannual variability in net $CO_2$ exchange of a native tallgrass prairie, Global Change Biol., 9, 255–265, doi:10.1046/J.1365-2486.2003.00567.X, 2003.

Tang, X. G., Wang, Z. M., Liu, D. W., Song, K. S., Jia, M. M., Dong, Z. Y., Munger, J. W., Hollinger, D. Y., Bolstad, P. V., Goldstein, A. H., Desai, A. R., Dragoni, D., and Liu, X. P.: Estimating the net ecosystem exchange for the major forests in the northern United States by integrating MODIS and AmeriFlux data, Agric. For. Meteorol., 156, 75–84, doi:10.1016/j.agrformet.2012.01.003, 2012.

US EPA: Inventory of US Greenhouse Gas Emissions and Sinks: 1990–2012, Washington, DC, 529 pp., 2014.

Ussiri, D. A. N., Lal, R., and Jarecki, M. K.: Nitrous oxide and methane emissions from long-term tillage under a continuous

corn cropping system in Ohio, Soil Till. Res., 104, 247–255, doi:10.1016/J.Still.2009.03.001, 2009.

Vesala, T., Kljun, N., Rannik, Ü., Rinne, J., Sogachev, A., Markkanen, T., Sabelfeld, K., Foken, T., and Leclerc, M.: Flux and concentration footprint modelling: State of the art, Environ. Pollut., 152, 653–666, 2008.

Werner, C., Davis, K., Bakwin, P., Yi, C. X., Hurst, D., and Lock, L.: Regional-scale measurements of $CH_4$ exchange from a tall tower over a mixed temperate/boreal lowland and wetland forest, Global Change Biol., 9, 1251–1261, 2003.

West, T. O., Bandaru, V., Brandt, C. C., Schuh, A. E., and Ogle, S. M.: Regional uptake and release of crop carbon in the United States, Biogeosciences, 8, 2037–2046, doi:10.5194/bg-8-2037-2011, 2011.

Williams, I. N., Riley, W. J., Torn, M. S., Berry, J. A., and Biraud, S. C.: Using boundary layer equilibrium to reduce uncertainties in transport models and $CO_2$ flux inversions, Atmos. Chem. Phys., 11, 9631–9641, doi:10.5194/acp-11-9631-2011, 2011.

Wunch, D., Wennberg, P. O., Toon, G. C., Keppel-Aleks, G., and Yavin, Y. G.: Emissions of greenhouse gases from a North American megacity, Geophys. Res. Lett., 36, L15810, doi:10.1029/2009gl039825, 2009.

Xiao, J. F., Zhuang, Q. L., Baldocchi, D. D., Law, B. E., Richardson, A. D., Chen, J. Q., Oren, R., Starr, G., Noormets, A., Ma, S. Y., Verma, S. B., Wharton, S., Wofsy, S. C., Bolstad, P. V., Burns, S. P., Cook, D. R., Curtis, P. S., Drake, B. G., Falk, M., Fischer, M. L., Foster, D. R., Gu, L. H., Hadley, J. L., Hollinger, D. Y., Katul, G. G., Litvak, M., Martin, T. A., Matamala, R., McNulty, S., Meyers, T. P., Monson, R. K., Munger, J. W., Oechel, W. C., U, K. T. P., Schmid, H. P., Scott, R. L., Sun, G., Suyker, A. E., and Torn, M. S.: Estimation of net ecosystem carbon exchange for the conterminous United States by combining MODIS and AmeriFlux data, Agric. For. Meteorol., 148, 1827–1847, doi:10.1016/j.agrformet.2008.06.015, 2008.

Yi, C., Davis, K. J., Bakwin, P. S., Berger, B. W., and Marr, L. C.: Influence of advection on measurements of the net ecosystem-atmosphere exchange of $CO_2$ from a very tall tower, J. Geophys. Res.-Atmos., 105, 9991–9999, doi:10.1029/2000jd900080, 2000.

Yi, C., Davis, K. J., Bakwin, P. S., Denning, A. S., Zhang, N., Desai, A., Lin, J. C., and Gerbig, C.: The observed covariance between ecosystem carbon exchange and atmospheric boundary layer dynamics at a site in northern Wisconsin, J. Geophys. Res., 109, D08302, doi:10.1029/2003JD004164, 2004.

Yi, C. X., Davis, K. J., Berger, B. W., and Bakwin, P. S.: Long-term observations of the dynamics of the continental planetary boundary layer, J. Atmos. Sci., 58, 1288–1299, doi:10.1175/1520-0469(2001)058<1288:Ltootd>2.0.Co;2, 2001.

Zhang, X.: Improving regional-scale greenhouse gas inventories in an agriculture-dominated landscape using a multi-scale approach, PhD Dissertation, Yale University, 2013.

Zhang, X., Lee, X., Griffis, T., Baker, J., Erickson, M., Hu, N., and Xiao, W.: The influence of plants on atmospheric methane in an agriculture-dominated landscape, Int. J. Biometeorol., 1–15, doi:10.1007/s00484-013-0662-y, 2013.

Zhang, X., Lee, X., Griffis, T., Andrews, A., Baker, J., Erickson, M., Hu, N., and Xiao, W.: Quantifying nitrous oxide fluxes on multiple spatial scales in the Upper Midwest, USA, Int. J. Biometeorol., 1–15, doi:10.1007/s00484-014-0842-4, 2014.

Zhao, C. F., Andrews, A. E., Bianco, L., Eluszkiewicz, J., Hirsch, A., MacDonald, C., Nehrkorn, T., and Fischer, M. L.: Atmospheric inverse estimates of methane emissions from Central California, J. Geophys. Res.-Atmos., 114, doi:10.1029/2008jd011671, D16302, 2009.

Zhuang, Q. L., Lu, Y. Y., and Chen, M.: An inventory of global $N_2O$ emissions from the soils of natural terrestrial ecosystems, Atmos. Environ., 47, 66–75, doi:10.1016/j.atmosenv.2011.11.036, 2012.